

Quantitative Subcellular Imaging of Glucose Metabolism within Intact Pancreatic Islets*

(Received for publication, September 20, 1995, and in revised form, November 9, 1995)

Brian D. Bennett‡, Thomas L. Jetton, Guangtao Ying, Mark A. Magnuson, and David W. Piston§

From the Department of Molecular Physiology and Biophysics, Vanderbilt University, Nashville, Tennessee 37232

Studies of dispersed β cells have been used to infer their behavior in the intact pancreatic islet. When dispersed, β cells exhibit multiple metabolic glucose-response populations with different insulin secretion properties. This has led to a model for glucose-dependent insulin secretion from the islet based on a step-wise recruitment of individual β cells. However, previously reported synchronous and uniform Ca^{2+} activity and electrical responses indicate that β cell behavior within intact islets is more uniform. Therefore, uncertainty remains whether β cell metabolic heterogeneity is functionally important in intact islets. We have used two-photon excitation microscopy to measure and compare the glucose-induced NAD(P)H autofluorescence response in dispersed β cells and within intact islets. Over 90% of β cells in intact islets responded to glucose with significantly elevated NAD(P)H levels, compared with less than 70% of dispersed β cells. In addition, all responding β cells within intact islets exhibited a sigmoidal glucose dose response behavior with inflection points of ~ 8 mM glucose. These results suggest that β cell heterogeneity may be functionally less important in the intact islet than has been predicted from studies of dispersed β cells and support the role of glucokinase as the rate-limiting enzyme in the β cell glucose response.

Insulin secretion from pancreatic β cells is tightly coupled to glucose metabolism (1–4). When dispersed, marked variability in the metabolic responses of β cells to glucose has been observed (5, 6) using NAD(P)H autofluorescence as an index of the cellular redox state (7). Based on this, it has been suggested that metabolic heterogeneity plays a fundamental role in whole islet insulin secretion by a mechanism of variable activation thresholds of individual β cells (8). The observation that glucokinase, which has been postulated as the rate-limiting step in glucose transduction by β cells (3), exhibits heterogeneous immunoreactivity among β cell also supports this model (9). However, other indicators of β cell function within intact islets, such as synchronous intracellular $[\text{Ca}^{2+}]_i$ (10) and electrical (11) responses, indicate that intraislet β cells constitute a functionally more homogeneous population. Direct measurement of the

metabolic behavior of cells within the intact islet, however, has not been performed. Here we report the first measurement of glucose-induced NAD(P)H autofluorescence changes within the intact islet at subcellular resolution using TPME¹ (12, 13). Using the same instrument, we also measured the glucose-induced metabolic behavior of isolated cells, thereby allowing a quantitative comparison of the metabolic response of β cells under both conditions.

A new alternative to confocal microscopy, TPME allows collection of optical sections within thick samples, such as pancreatic islets, with greatly reduced photobleaching and photodamage. Previously, we have described a laser scanning microscope that is optimized for TPME of UV excitable fluorophores, such as NAD(P)H (14). This instrument allows extended dynamic studies of many cells simultaneously, thereby permitting observation of the temporal and spatial organization of metabolic activity within the intact islet.

EXPERIMENTAL PROCEDURES

Islet Isolation and Culture—Rat islets were isolated by pancreatic distention followed by collagenase digestion (15). Only the splenic portion of the pancreas was digested in order to select an islet population enriched in α cells over δ and PP cells (16). Rats were treated under protocols approved by the Vanderbilt University Animal Care Committee. Before imaging, islets were cultured for 1–5 h in RPMI 1640 medium (Life Technologies, Inc.) containing 10% fetal bovine serum (Life Technologies, Inc.), 100 IU/ml penicillin, and 100 $\mu\text{g}/\text{ml}$ streptomycin. For imaging, islets were attached to a coverslip with Cell-Tak (Collaborative Biomedical Products, Bedford, MA), and the coverslip was placed in a temperature-controlled perfusion micro incubator (TLC-MI, Adam and List Associates, Westbury, NY). This micro incubator held the temperature of the sample at 37 °C (measured by thermocouple adjacent to the islet) by heating both the coverslip chamber and incoming perfusate. An air stream incubator (Nicholson Precision Instruments, Gaithersburg, MD) heated the objective to the perfusate temperature to eliminate heat transfer through the oil-glass objective interface. Individual islet cells were dispersed by the method of Pralong *et al.* (17) except that 15–25 islets were exposed to 50 μl of calcium-free 25 $\mu\text{g}/\text{ml}$ trypsin solution for 5 min. Cells were titrated briefly and plated onto marked coverslips (Bellco) coated with a monolayer of Cell-Tak.

Quantitative NAD(P)H Imaging in Living Islets and Isolated β Cells—Two-photon excitation microscopy was performed using a previously described instrument (14). Briefly, a 76-MHz train of 100 femtosecond pulses of 710-nm light from a mode-locked Ti:Sapphire laser (Coherent Mira, Mountain View, CA) was focused on to the sample by a 40 \times , 1.3 NA Plan Neofluar objective lens (Carl Zeiss, Thornwood, NY). The focal volume, the only region where fluorophore excitation occurs because of the intensity-squared dependence of the two-photon absorption, was raster scanned to build a 150 \times 150 \times 1- μm optical section. Autofluorescence from the sample (400–550 nm) was collected by the objective, separated from the excitation light by a dichroic mirror (550 DCLP Ext R, ChromaTechnology, Brattleboro, VT), filtered to remove scattered red light (550 SP with blocking from 700 to 750 nm, ChromaTechnology), and directed to a photomultiplier tube detector (Hamamatsu R268). Output from the detector was integrated, stored,

* These studies were supported by funds from the Beckman Foundation Young Investigator Program (to D. W. P.), by a Pilot and Feasibility award from the Vanderbilt Diabetes Research and Training Center (to D. W. P.), and by National Institutes of Health Grants DK42612 and DK42502 (to M. A. M.). The costs of publication of this article were defrayed in part by the payment of page charges. This article must therefore be hereby marked “advertisement” in accordance with 18 U.S.C. Section 1734 solely to indicate this fact.

‡ Supported by the National Institutes of Health Multidisciplinary Training Program in Molecular Endocrinology.

§ To whom correspondence should be addressed: Dept. of Molecular Physiology and Biophysics, Vanderbilt University, 702 Light Hall, Nashville, TN 37232. Tel.: 615-322-7030; Fax: 615-322-7236; E-mail: dave.piston@mcmail.vanderbilt.edu.

¹ The abbreviations used are: TPME, two-photon excitation microscopy; PBS, phosphate-buffered saline.

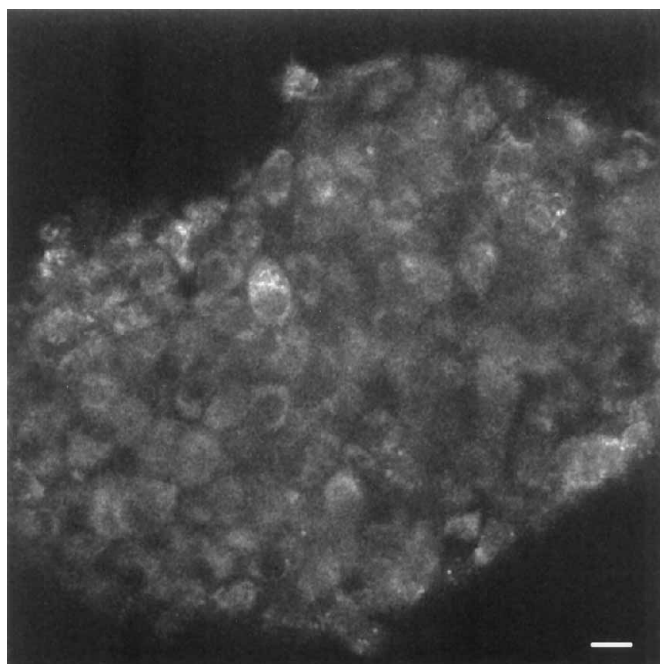


FIG. 1. **NAD(P)H autofluorescence in an optical section of an isolated rat islet.** Individual β cells and their nuclei are visible 40 μm into an islet mounted on a coverslip. The reduced light scattering and absorption associated with TPEM (red light instead of UV light is used to excite NAD(P)H) affords unprecedented clarity in optical sections throughout the islet. The scale bar is 10 μm .

and displayed by computer.

For the dynamic NAD(P)H images, the perfusion was turned off, image acquisition was started, and 8 s later a small volume of test agent was added at the far edge of the sample chamber, which initially contained 3 ml of basal buffer (DME base (Sigma) with 2 mM glutamine and 1 mM glucose). In these experiments, it was more convenient to use a glass-bottomed 35-mm dish (PG35G-0-14-gm, Matek Corporation, Ashland, MA) than the coverslip chamber, but temperature was still maintained by heating both the stage and the objective lens. Pre-heated test solutions were added as follows: 100 μl of 1 M glucose, 60 μl of 1 M mannoheptulose, or 100 μl 100 mM NaCN to give the approximate final concentrations of 30, 20, and 3 mM, respectively. TPEM images were acquired continuously for 136 s at 8 s/scan.

For the steady-state glucose response measurements, islets were perfused at 1.2 ml/min and 37 $^{\circ}\text{C}$ with Krebs-Ringer bicarbonate buffer (120 mM NaCl, 4.8 mM KCl, 2.5 mM CaCl_2 , 1.2 mM MgCl_2 , 5 mM NaHCO_3 , and 10 mM HEPES, pH 7.4) containing 3, 5, 7.5, 12, or 23 mM glucose, and NAD(P)H autofluorescence was measured after 10 min of equilibration with each different concentration of glucose. In a parallel experiment using 12 mM glucose, images acquired at 5-min intervals after the addition of glucose, showed that 10 min was sufficient to reach the response plateau.

NAD(P)H measurements of dispersed cells were performed by the same techniques as the glucose response, except that perfusion rate was lowered to 0.5 ml/min and glucose levels were varied between 1 mM and 30 mM to compare directly with the dynamic NAD(P)H measurements in whole islets.

Immunofluorescence and Confocal Microscopy— β and α cells were identified by insulin and glucagon immunostaining, respectively. After measuring the autofluorescence responses by TPEM, islets were fixed in 4.0% paraformaldehyde in 10 mM PBS for 1 h at 4 $^{\circ}\text{C}$, washed in three changes of PBS for 20 min each, and then permeabilized in PBS containing 0.3% Triton X-100 for 3 h at room temperature. This solution was replaced with 1:1 permeabilization solution and 5% normal donkey serum in PBS for 8 h. Following blocking, this solution was replaced with antibody dilution buffer (PBS + 0.2% Triton + 1.0% bovine serum albumin) for 20 min followed by fresh antibody dilution buffer (~1.0 ml). Primary antisera were added at final dilutions of 1:1000 each for guinea pig anti-insulin IgG (Linco Research Inc.) and rabbit anti-glucagon IgG (ICN Biologicals). Following incubation for 8 h, islets were washed in four changes of wash buffer (PBS + 0.2% Triton) for 30 min each. Antibody dilution buffer was then added with 4 $\mu\text{g}/\text{ml}$ of "ML" grade donkey anti-guinea pig IgG-CY3 and 5 $\mu\text{g}/\text{ml}$ of donkey anti-

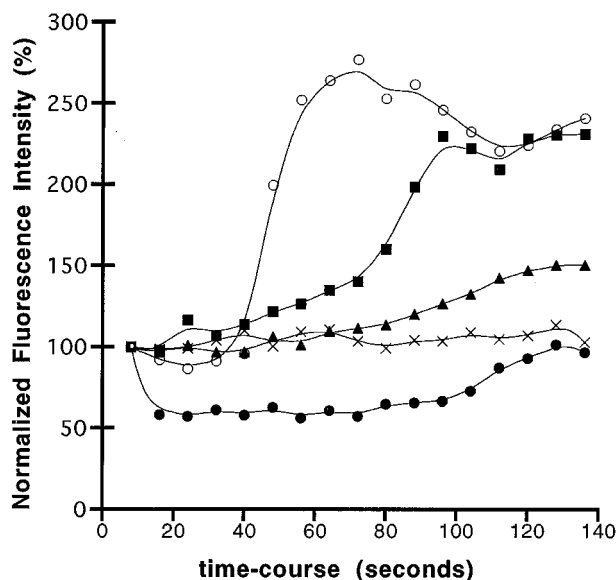


FIG. 2. **Cellular autofluorescence detected in islets by TPEM is due to NAD(P)H.** Digital image analysis was used to measure autofluorescence in single β cells after image acquisition. NaCN (3 mM), which inhibits cellular respiration, caused a >2.5-fold rise in cellular autofluorescence (○, $n = 5$ islets). Mannoheptulose (20 mM), which inhibits glucose utilization by competitive inhibition of glucokinase, resulted in a ~50% decrease in autofluorescence (●, typical β cell, $n = 3$ islets). Glucose stimulation (30 mM) increased autofluorescence >2-fold (■, typical β cell, $n = 8$ islets). An average laser power of 3 mW at the sample produced NAD(P)H autofluorescence signals adequate for imaging without detectable photobleaching (×). Continuous exposure to excessive doses of two-photon irradiation (>5 mW average power) caused a 1.5-fold increase in autofluorescence after 136 s (▲). This cellular photodamage was caused by two-photon interactions because islets pre-exposed to 15 mW of defocused red light showed no change in NAD(P)H levels (data not shown). The scale bar is 10 μm .

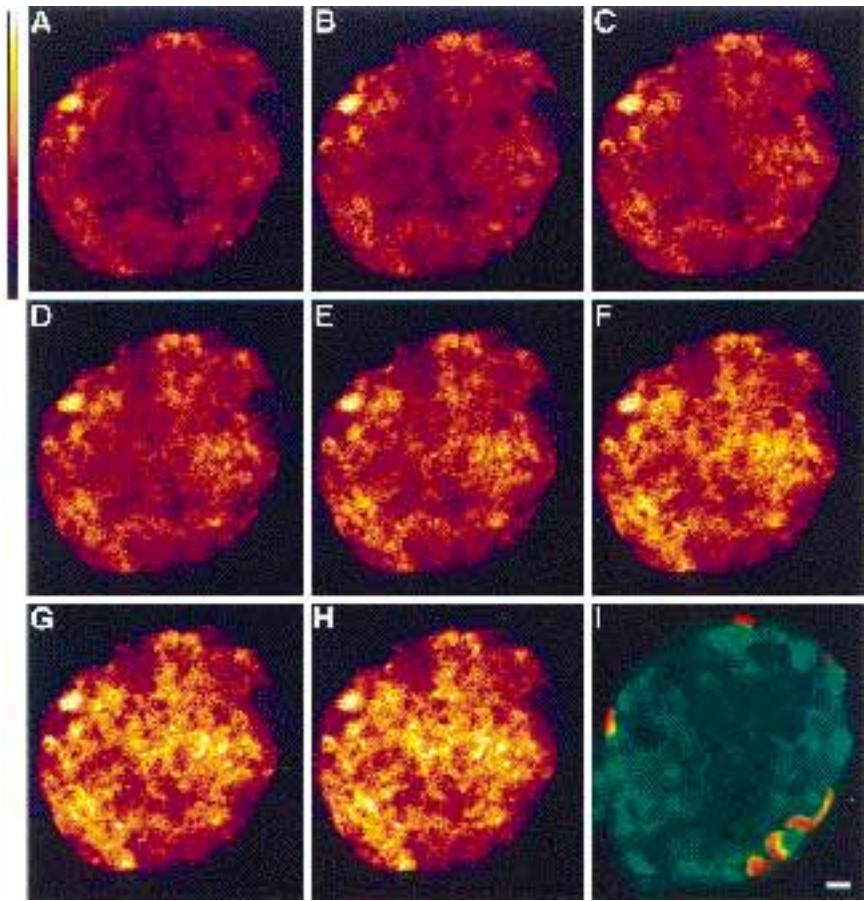
rabbit IgG-FITC (Jackson ImmunoResearch) and incubated for 8 h. Following washing, islets were mounted in Aqua-Polymount (Polysciences, Inc.) and imaged sequentially for insulin and glucagon using the 543- and 488-nm lines of a HeNe and Ar-Kr laser, respectively, with a Zeiss LSM 410 confocal microscope. Dispersed β cells were identified in the same manner, with the marked coverslip allowing easy correlation of cells between the NAD(P)H and immunofluorescence images.

Digital Image Analysis—Digital image processing of time series was performed on a Macintosh Power PC 6100AV computer running Alice (Perceptive Systems, Inc., Boulder, CO) using the "Particle Series" custom add-on. Means were taken in 25 pixel circular regions of interest in the cytoplasm of single islet cells to generate a time course or glucose response for NAD(P)H autofluorescence. The traces shown are each representative of at least 30 cells analyzed in this manner.

RESULTS

We have measured NAD(P)H autofluorescence at the subcellular level throughout intact pancreatic islets (Fig. 1) by combining TPEM (14) with established quantitative laser scanning microscopy methods (18). Subcellular structures, such as the nuclei (which appear dark in the NAD(P)H image) are clearly visible. The spatial discrimination and collection efficiency are sufficient to quantitatively assess NAD(P)H levels in individual β cells, with temporal resolutions of 4–8 s/image. A series of control experiments were performed to demonstrate that the fluorescence changes observed were due to changes in [NAD(P)H] and to establish the limits of islet viability during TPEM (Fig. 2). Inhibition of respiration using cyanide produced about a 2-fold elevation in autofluorescence, whereas inhibition of glucose phosphorylation with mannoheptulose led to a ~50% reduction. The effect of these metabolic perturbations on NAD(P)H levels agrees with similar measurements using UV excitation (7, 19). Laser irradiation of ~3 mW (average power at the sample) generated signals sufficient for imaging without

FIG. 3. Serial images showing the temporal metabolic responses of cells visible in an optical section of an intact islet. Two-photon excitation of cellular autofluorescence is shown in A–H. After measuring dynamic changes, β and α cells (I, green for insulin and red for glucagon) were identified by immunofluorescent staining and confocal microscopy. The NAD(P)H images shown (time course generated as in Fig. 2) begin one scan before any increase was detected and continue at 8-s intervals thereafter. NAD(P)H autofluorescence began to increase in peripheral cells 32 s after glucose addition (B) and then spread inward toward the center of the islet (C–H). Peak NAD(P)H autofluorescence in central β cells lagged that of the periphery by about 40 s, consistent with glucose diffusion into the islet.



evidence of cellular damage (e.g. autofluorescence increase, detectable photobleaching, or degradation of glucose response). However, extended laser irradiation >5 mW resulted in increased autofluorescence (Fig. 2) and the loss of any glucose-induced autofluorescence response (data not shown). To determine if the laser-induced autofluorescence increase was caused by two-photon excitation or the incident red light, islets were exposed to intense laser illumination focused into the coverslip. This exposed the entire islet to unfocused red light without generating any two photon excitation within cells. In this situation, even 15 mW of unfocused red light did not affect autofluorescence, and the subsequent glucose-induced NAD(P)H response was unaffected. Thus, islet cells are sensitive only to the amount of two-photon excitation and not single-photon interactions from the red light.

To allow quantitative comparison of cells in the intact islet and after dispersion, we measured NAD(P)H responses of cells in both situations. In the case of intact islets, dynamic behavior was also observed over several successive images. The temporal metabolic response to glucose of a single optical section of cells in an intact islet is shown in Fig. 3 (A–H). To attribute responses to specific islet cell types after TPDM, β and α cells were identified by retrospective immunofluorescent staining and conventional laser scanning confocal microscopy (Fig. 3I, green for insulin and red for glucagon).

Increased NAD(P)H autofluorescence was observed ~ 32 s after switching from low to high glucose. The increase was observed first at the islet periphery with a gradual spread of the autofluorescence response to the central β cells about 40 s later, consistent with glucose diffusion into the islet. Except for this time delay, the NAD(P)H autofluorescence increase of all β cells was strikingly uniform. Some cells began and ended the experiment with relatively low autofluorescence, thus giving

the appearance of heterogeneity in single images. However, these cells showed a proportionate increase in NAD(P)H, which could be readily detected by animation (rapid playback of time series images, animation is available by World Wide Web at <http://160.129.157.26>) and could be quantitated by digital image analysis of single cells (see below). In α cells, the NAD(P)H signal did not increase in response to increased glucose; these cells were excluded from further analysis.

To quantitatively assess the metabolic response of the intra-islet β cell population, we determined the ratio of peak NAD(P)H signal/initial NAD(P)H signal for every β cell present in single optical sections from five islets (46–133 β cells/islet section). The average β cell response ratio in a single islet section ranged from 1.74 to 2.45 (for the five islets studied), each with a standard deviation $<25\%$ of the mean. To compare these results to isolated β cells, nonresponding β cells were defined as those that showed responses less than two standard deviations below the mean. By this measure, nonresponding β cells in five islets constituted 14, 6, 13, 5, and 6% (mean = 9%) of insulin immunopositive cells. A similar result was obtained when nonresponding cells were identified and counted by animation. By either method, all of the nonresponding β cells were located at the periphery of the islet.

Measurements of NAD(P)H levels at various steady-state glucose concentrations were performed to further examine responses at the single-cell level in intact islets (Fig. 4). The response curves generated from eight typical β cells within two intact islets, which are shown in Fig. 4, are sigmoidal with inflection points at ~ 8 mM glucose. This dose response behavior is consistent with the rate-limiting role of glucokinase, the high K_m hexokinase in the β cell (3, 20, 21).

To validate the results obtained from intact islets, we also examined the NAD(P)H response of isolated β cells. Fig. 5

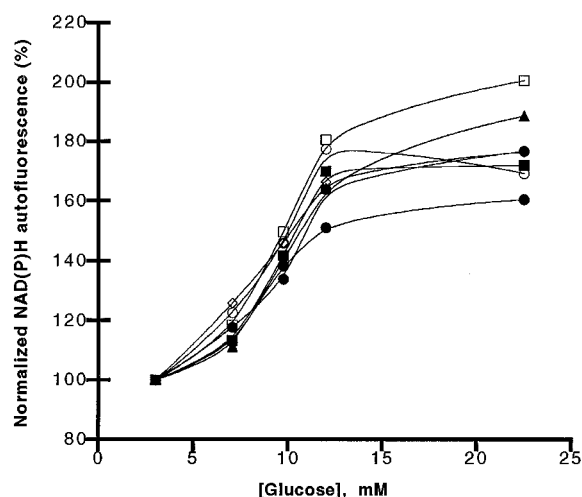


FIG. 4. **Metabolic response measurement within intact islets at steady-state glucose concentrations.** These sigmoidally shaped glucose concentration-dependent response curves were obtained. The inflection point at 8 mM is consistent with a rate-limiting role for glucokinase in β cell glucose usage (3). These response curves were taken from eight representative cells across two separate islet preparations.

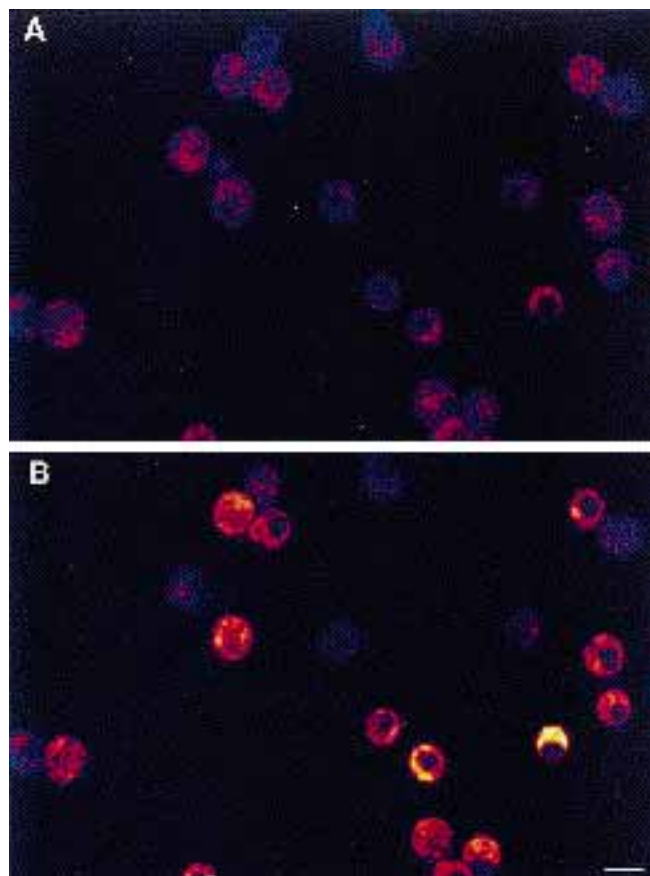


FIG. 5. **NAD(P)H autofluorescence measured by TPEM in isolated β cells.** The responses of these dissociated cells as glucose is increased from 1 (A) to 30 mM (B) are much more heterogeneous than those of β cells in intact islets. The scale bar is 12 μ m.

shows a typical field of dissociated islet cells in the presence of 1 mM (Fig. 5A) or 30 mM glucose (Fig. 5B). As with intact islets, retrospective immunostaining was performed to confirm that all analyzed cells were β cells. Parallel control experiments on the same cell preparations showed that $>95\%$ of the cells were viable as determined by either trypan blue exclusion (negative control for membrane integrity) or Fura-2/AM uptake (positive

control for esterase activity). As seen in all fields of dispersed β cells, Fig. 5 shows much greater variability in the NAD(P)H response to glucose than the intact islets (equivalent images are shown in Fig. 3, A and H). The mean NAD(P)H autofluorescence increase for dispersed β cells was ~ 1.9 (similar to that seen in whole islets), but the standard deviation of the increase was $\sim 35\%$ of the mean (greater variation than the 25% observed in intact islets). The percentage of nonresponding isolated β cells was also quantified using the same definitions as in the intact islets. This analysis showed that 17 of 53 ($\sim 32\%$) dispersed β cells, obtained from two separate islet preparations, were found to be nonresponsive.

DISCUSSION

We have used two-photon excitation microscopy to measure and compare the metabolic responses to glucose of individual cells within intact pancreatic islets. We confirmed that the observed autofluorescence was largely due to NAD(P)H because its responses to cyanide and mannoheptulose exposure were consistent with those from established techniques on isolated β cells (7, 22). Measurement of NAD(P)H autofluorescence in an intact pancreatic islet requires a sophisticated technique, such as TPEM, because of the tissue thickness and high levels of fluorescence background. Whole islet experiments were possible because the lack of out-of-focus fluorescence generation inherent in two-photon imaging allowed acquisition of optical sections deep within the islets (Fig. 1). Although NAD(P)H is a very poor fluorophore, having both a low absorption cross-section and quantum yield, TPEM enabled extended time course measurements without measurable photobleaching and photodamage. This allowed continuous NAD(P)H imaging of a single islet for several minutes without killing the cells (Fig. 2). Even using TPEM, however, there is always a trade-off between the signal to noise ratio and temporal resolution (13), and in order to obtain sufficient signal for these NAD(P)H autofluorescence measurements, we were usually limited to 8 s/image.

The glucose-induced metabolic responses from the β cells in intact islets were strikingly uniform and contrast significantly with the heterogeneous behavior of isolated β cells (Figs. 3 and 5). In our experiments, greater than 90% of β cells in intact islets were metabolically active, whereas less than 70% of dispersed β cells responded to the same glucose concentrations. These isolated cell measurements are in excellent agreement with previous reports where the metabolically responsive population of isolated β cells in the presence of 20 mM glucose was determined to be 70% (5, 8). In addition, as shown in Fig. 5, the amplitude of response varied more greatly in the dispersed cells.

Two explanations for the differences observed between isolated cells and those in the intact islet seem possible, and each has different implications. The first explanation is that proteolytic damage during islet and single-cell isolation procedures may degrade the NAD(P)H response of certain cells without compromising their viability. In intact islets, all nonresponsive cells were at the periphery, and cells on the islet exterior would obviously be more prone to this kind of damage. A similar damage mechanism may also be responsible for the increased fraction of nonresponsive dispersed β cells, because islet dispersion requires even more aggressive proteolytic treatment. If this is the case, then models developed from studies of isolated β cells are unlikely to accurately describe islet function.

A second explanation for the differences between isolated β cells and those in intact islets could be that intercellular communication might act to overcome the heterogeneities of individual β cells. Cell-cell contact may allow less responsive cells to be entrained by the more responsive cells, but this was not

observed in the dissociated cells (Fig. 5) where cells in contact were not found to respond more uniformly than completely isolated ones. In intact islets, individual β cells never displayed earlier responses than neighboring cells (Fig. 3), so any entrainment mechanism would need to act faster than a few seconds. Such coupling cannot be electrical because electrophysiological and $[\text{Ca}^{2+}]_i$ measurements show a time lag between the NAD(P)H increase and membrane depolarization of >15 s (23). Such a mechanism would likely involve a small, easily diffusible messenger. This messenger could also diffuse rapidly toward the islet core and generate an activation signal ahead of the primary glucose-induced autofluorescence wave, but no such signal was observed (Fig. 3). Although it may be possible to construct a model with a messenger that can equilibrate between adjacent cells within a few seconds and not trigger cells toward the islet center sooner than the measured 40 s delay, we conclude that such an entrainment mechanism is unlikely.

In the absence of a defined entrainment mechanism, the uniform metabolic response results in the whole islet appear to be inconsistent with significant metabolic heterogeneity among β cells, but the images do show autofluorescence heterogeneity at the initial glucose concentration of 1 mM (Fig. 3A), as do the isolated β cells (Fig. 5A). This basal autofluorescence heterogeneity suggests that a metabolic thresholding based on the absolute ATP/ADP ratio (related to the absolute NAD(P)H/NAD(P)⁺ ratio) could generate heterogeneous β cell function even in the presence of a uniform NAD(P)H response. However, such basal heterogeneities in whole islets are difficult to interpret, because they could possibly arise due to variable optical density or the subcellular distribution of NAD(P)H. First, cells in the middle of the islet generally have more tissue between them and the objective lens than do cells on the periphery, and more fluorescence signal is indeed detected in the peripheral cells (Fig. 3). Secondly, because the 1- μm -thick optical section passes through each cell differently, the amount of NAD(P)H detected in each cell may differ as well.

The metabolic heterogeneity found in dispersed β cells has been shown to correlate with heterogeneity in insulin secretion and has thus led to a model for islet function based on variable activation thresholds (8). However, our measurements of NAD(P)H changes as a function of glucose concentration indicated a sigmoidal dose response with an inflection point at ~ 8 mM glucose (Fig. 4). This coincides with the K_m of glucokinase, the β cell glucose sensor (3, 21), and contradicts a model where the sigmoidal insulin secretory response from the whole islet is generated by a stepwise recruitment of individual β cells with

variable activation thresholds (8). None of the β cells examined here exhibited different inflection points, as would be predicted by the stepwise recruitment model. We conclude that a stepwise recruitment of β cells does not describe insulin secretion from whole islets. However, in the absence of direct insulin secretion measurements from individual cells within the islet, models of functional heterogeneity cannot be ruled out. The results may also be inconsistent with previous descriptions of pronounced β cell glucokinase heterogeneity as detected by immunohistochemical methods (9). Further studies of the differences between intact islet and isolated β cells using TPTEM should lead to a resolution of these controversies and a greater understanding of intraislet metabolic response dynamics.

Acknowledgments—Confocal microscopy was performed at the Vanderbilt Cell Imaging Resource. We thank V. Blackwell and S. Knobel for technical assistance.

REFERENCES

1. Matschinsky, F. M., and Ellerman, J. E. (1968) *J. Biol. Chem.* **243**, 2730–2736
2. Coore, H. G., and Randle, P. J. (1964) *Biochem. J.* **93**, 66–78
3. Matschinsky, F., Liang, Y., Kesavan, P., Wang, L., Froguel, P., Velho, G., Cohen, D., Permutt, M. A., Tanizawa, Y., Jetton, T. L., Niswender, K., and Magnuson, M. A. (1993) *J. Clin. Invest.* **92**, 2092–2098
4. Randle, P. J. (1993) *Diabetologia* **36**, 269–274
5. Kiekens, R., In't Veld, P., Schuit, F., Van De Winkel, M., and Pipeleers, D. (1992) *J. Clin. Invest.* **89**, 117–125
6. Van Schravendijk, C. F. H., Kiekens, R., and Pipeleers, D. G. (1992) *J. Biol. Chem.* **267**, 21344–21348
7. Balaban, R. S., and Mandel, L. J. (1990) in *Noninvasive Techniques in Cell Biology* (Foskett, J. K., and Grinstein, S., eds) pp. 213–236, Wiley-Liss, New York
8. Pipeleers, D., Kiekens, R., Ling, Z., Wilkens, A., and Schuit, F. (1994) *Diabetologia* **37**, S57–S64
9. Jetton, T. L., and Magnuson, M. A. (1992) *Proc. Natl. Acad. Sci. U. S. A.* **89**, 2619–2623
10. Santos, R. M., Rosario, L. M., Nadal, A., Garcia, S. J., Soria, B., and Valdeolmillos, M. (1991) *Pfluegers Arch. Eur. J. Physiol.* **418**, 417–422
11. Meda, P., Atwater, I., Goncalves, A., Bingham, A., Orci, L., and Rojas, E. (1984) *Q. J. Exp. Physiol.* **69**, 719–735
12. Denk, W., Strickler, J. H., and Webb, W. W. (1990) *Science* **248**, 73–76
13. Denk, W., Piston, D. W., and Webb, W. W. (1995) in *Handbook of Biological Confocal Microscopy*, (Pawley, J., ed) 2nd Ed., pp. 445–458, Plenum Publishing Corp., New York
14. Piston, D. W., Bennett, B. D., and Ying, G. (1995) *J. Microsc. Soc. Am.* **1**, 25–34
15. Sharp, D. W., Kemp, C. B., Knight, M. J., Ballinger, W. F., and Lacy, P. F. (1973) *Transplantation* **16**, 686–689
16. Stefan, Y., Meda, P., Neufeld, M., and Orci, L. (1987) *J. Clin. Invest.* **80**, 175–183
17. Pralong, W. F., Bartley, C., and Wollheim, C. B. (1990) *EMBO J.* **9**, 53–60
18. Sandison, D. R., Williams, R. M., Wells, K. S., Strickler, J. S., and Webb, W. W. (1995) in *Handbook of Biological Confocal Microscopy* (Pawley, J., ed) 2nd Ed., pp. 39–54, Plenum Publishing Corp., New York
19. Gilon, P., and Henquin, J. C. (1992) *J. Biol. Chem.* **267**, 20713–20720
20. Malaisse, W. J. (1991) in *The Endocrine Pancreas* (Samols, E., ed) pp. 73–92, Raven Press, Ltd., New York
21. Matschinsky, F. M. (1990) *Diabetes* **39**, 647–652
22. Henquin, J. C. (1990) *Pfluegers Arch. Eur. J. Physiol.* **416**, 568–572
23. Duchon, M. R., Smith, P. A., and Ashcroft, F. M. (1993) *Biochem. J.* **294**, 35–42